Reactivity of Horseradish Peroxidase Compound II toward Substrates: Kinetic Evidence for a Two-Step Mechanism†

José Neptuno Rodríguez-López,‡ María Angeles Gilabert,‡ José Tudela,‡ Roger N. F. Thorneley,§ and Francisco García-Cánovas*,‡

Grupo de Investigación de Enzimología (GENZ), Departamento de Bioquímica y Biología Molecular-A, Facultad de Biología, Universidad de Murcia, E-30100 Espinardo, Murcia, Spain, and Department of Biological Chemistry, John Innes Centre, NR4 7UH Norwich, U.K.

Received May 22, 2000; Revised Manuscript Received August 3, 2000

ABSTRACT: Transient kinetic analysis of biphasic, single turnover data for the reaction of 2,2′-azino-bis-[3-ethylbenzthiazoline-6-sulfonic acid] (ABTS) with horseradish peroxidase (HRPC) compound II demonstrated preequilibrium binding of ABTS ($k_{+5} = 7.82 \times 10^4$ M^{-1} s^{-1}) prior to rate-limiting electron transfer ($k_{+6} = 42.1$ s^{-1}). These data were obtained using a stopped-flow method, which included ascorbate in the reaction medium to maintain a low steady-state concentration of ABTS (pseudo-first-order conditions) and to minimize absorbance changes in the Soret region due to the accumulation of ABTS cation radicals. A steady-state kinetic analysis of the reaction confirmed that the reduction of HRPC compound II by this substrate is rate-limiting in the complete peroxidase cycle. The reaction of HRPC with *o*-diphenols has been investigated using a chronometric method that also included ascorbate in the assay medium to minimize the effects of nonenzymic reactions involving phenol-derived radical products. This enabled the initial rates of *o*-diphenol oxidation at different hydrogen peroxide and *o*-diphenol concentrations to be determined from the lag period induced by the presence of ascorbate. The kinetic analysis resolved the reaction of HRPC compound II with *o*-diphenols into two steps, initial formation of an enzyme−substrate complex followed by electron transfer from the substrate to the heme. With *o*-diphenols that are rapidly oxidized, the heterolytic cleavage of the O−O bond of the heme-bound hydrogen peroxide ($k_{+2} = 2.17 \times 10^3$ s^{-1}) is rate-limiting. The size and hydrophobicity of the *o*-diphenol substrates are correlated with their rate of binding to HRPC, while the electron density at the C-4 hydroxyl group predominantly influences the rate of electron transfer to the heme.

Peroxidases are ubiquitous in the plant and animal kingdoms (see ref *1* and references therein). The cationic isoenzyme from horseradish peroxidase (HRPC) has been intensively studied not least because of its commercial use in diagnostic assays and potential application in bioremediation (*2*−*5*). The normal peroxidase cycle for HRPC is shown in Scheme 1 (*6*) where HRPC-I and HRPC-II are the oxidized states of HRPC often referred to as compounds I and II, respectively. RH_2 is a reducing substrate, and $RH^{\bullet}$ is a free radical product. The catalytic cycle is initiated by a rapid ($k_a = 1.7 \times 10^7$ M^{-1} s^{-1}) $2e^-$ oxidation of the enzyme by hydrogen peroxide (or other organic peroxides) to give a green enzyme intermediate, HRPC-I, with the heme iron oxidized to the oxyferryl state [Fe(IV)═O] and a π-cation radical on the porphyrin ring. To complete a peroxidation cycle, HRPC-I is converted back to the resting enzyme Fe(III) state by two successive single electron-transfer reactions from reducing molecules; the first yielding a second enzyme intermediate, HRPC-II, which retains the oxyferryl group but not the porphyrin cation radical. Both of these reactions can yield free radical products that may undergo subsequent chemistry. The rate of the peroxidation cycle usually depends on the nature of the reducing substrate, with the reduction of HRPC-II to resting enzyme being rate-limiting (*7*). This model does not consider Michaelis−Menten complexes of ferric enzyme with H_2O_2 or of compounds I and II with reducing substrate since early experimental observations did not reveal evidence of saturation kinetics (*8*, *9*). This also implied that the peroxidase cycle is irreversible (*6*). However Wang et al. (*10*) recently reported clear kinetic evidence for a Michaelis−Menten complex between HRPC-II and the reducing substrate di-(*N*-acetyl-L-tyrosine).

Scheme 1

$$\text{HRPC} + H_2O_2 \xrightarrow{k_a} \text{HRPC-I} + H_2O$$

$$\text{HRPC-I} + RH_2 \xrightarrow{k_b} \text{HRPC-II} + RH^{\bullet}$$

$$\text{HRPC-II} + RH_2 \xrightarrow{k_c} \text{HRPC} + RH^{\bullet} + H_2O$$

Compound I formation has been widely studied and resolved into two reactions: the formation of an intermediate enzyme−peroxide complex followed by heterolytic cleavage of the oxygen−oxygen bond (*11*−*14*). His42 and Arg38, located in the distal heme cavity, are key residues that modulate both of these reactions (*13*−*16*). Although the

† This work was partly supported by a grant from the Ministerio de Educación y Cultura (Spain) Project PB98-0403-C02 and from the EU Human Capital and Mobility Programme "Peroxidases in Agriculture, the Environment and Industry" (Contract ERB FMRX-CT98-0200).

* To whom correspondence should be addressed (fax: 00-34-968-363963 or 00-34-968-364147; e-mail: canovasf@fcu.um.es).

‡ Universidad de Murcia.

§ John Innes Centre.

10.1021/bi001150p CCC: $19.00
Published on Web 10/06/2000

reactions of compounds I and II with some reducing substrates have been studied by stopped-flow spectrophotometry (*7*), there are experimental difficulties. The excess of substrate required for pseudo-first-order kinetics can increase the rate of the reaction beyond the range of stopped-flow methods ($k_{obs} > 10^3$ s^{-1}), and the formation of intensely colored products can make analysis of spectrophotometric data difficult. Thus, the value of the second-order rate constant for the reaction of HRPC-I with the common substrate 2,2′-azino-bis[3-ethylbenzthiazoline-6-sulfonic acid] (ABTS) (k_b in Scheme 1) was unknown until Goodwin et al. (*17*) developed a method that uses excess ascorbate to rapidly reduce substrate derived radicals. This keeps the concentration of the intensely colored ABTS radicals very low, thereby minimizing interference with the small absorbance changes associated with interconversion of different states of the heme. Steady-state kinetics has been used to study the peroxidase cycle (see ref *1* and references therein). However, since HRPC-I usually reacts considerably faster than HRPC-II with the reducing substrate, the rate constant for the former reaction cannot usually be determined. Smith et al. (*18*) deduced from a steady-state kinetic analysis that two first-order steps are needed to describe the reaction of HRPC-II with ABTS. Of these, the second step, the dissociation of the ABTS radical product from ferric enzyme, is rate limiting.

The oxidation of phenols by HRPC produces extremely reactive free radical intermediates which, following release from the enzyme, readily condense to yield polymeric products of variable stoichiometry. The kinetics of these reactions is not described by classical Michaelis−Menten equations. Saturation kinetics are often not observed because of the limited solubility of many of these substrates. In addition, the rates at which some substrates are oxidized are so high that they cannot be determined accurately, even with very low substrate concentrations. To our knowledge, there is very little evidence for the formation of a Michaelis−Menten complex between HRPC-II and a phenolic substrate (*10*, *19*). In this paper, we demonstrate for the first time that HRPC-II forms a Michaelis−Menten complex in its reaction with ABTS and *o*-diphenolic substrates. We have optimized methods based on the rapid reduction of free radical products by ascorbate for both pre-steady-state and steady-state kinetic measurements. The factors that determine the strength of binding and rate of oxidation of phenolic substrates by HRPC-II are also discussed.

MATERIALS AND METHODS

Reagents. HRP isoenzyme C was purchased from Sigma (type VI; Rz = 3.2) and used without further purification. The concentration of HRPC was determined spectrophotometrically using a Soret extinction coefficient of 102 mM^{-1} cm^{-1} (*20*). Reagent-grade H_2O_2 (30% v/v) was obtained from BDH/Merck (Poole, U.K.), and its concentration was calculated by iodide titration with HRPC (*21*). ABTS in the crystallized diammonium salt form, 4-methylcatechol, *N*-acetyldopamine, dopamine hydrochloride, epinine, L-isoproterenol, L-dopa, and L-α-methyldopa were purchased from Sigma (Madrid, Spain). 3,4-Dihydroxyphenylpropionic acid (DHPPA), 3,4-dihydroxyphenylacetic acid (DHPAA), L-noradrenaline hydrochloride, catechol, and 4-*tert*-butylcatechol were from Fluka (Madrid, Spain). Pyrogallol was from Aldrich (Madrid, Spain). L-Ascorbic acid was obtained from Sigma, and its concentration was determined by the lag period induced in the diphenolase activity of tyrosinase using L-dopa as substrate (*22*). Stock solutions of reducing substrates were prepared in 0.15 mM phosphoric acid to prevent autoxidation. All reagents and buffers were sparged with N_2. All other chemicals were of analytical grade and supplied by Merck (Germany). Milli-Q system (Millipore Corp.) ultrapure water was used throughout this research.

Pre-Steady-State Kinetics. Transient kinetics were monitored in a stopped-flow spectrophotometer (model SF-51, Hi Tech Scientific, Salisbury, U.K.). Data were recorded and analyzed on a PC running software provided by manufacturer. HRPC-II was prepared from the purified native enzyme by adding 1 equiv of H_2O_2 and 0.9 equiv of ascorbic acid. The maximum change in extinction on conversion of HRPC-II to native HRPC [$\Delta\epsilon_{423\,nm} = 95.3$ mM^{-1} cm^{-1} (*23*)] was used to monitor the reaction with ABTS in the presence of a 3-molar fold excess of ascorbic acid over reducing substrate. The rapid reduction of radical products by ascorbate ensures a constant substrate concentration (i.e., maintains pseudo-first-order conditions) and avoids the formation of colored products, such as ABTS cation radical (*17*). Temperature was controlled at 25 °C using a Techne C-400 circulating bath with a heater−cooler.

Steady-State Kinetics of the Reaction of HRPC with ABTS. Spectrophotometric measurements were made with a Perkin-Elmer Lambda-2 UV−visible spectrophotometer interfaced on-line with a PC-compatible computer. Steady-state kinetics were studied by measuring the initial rates of ABTS oxidation at 25 °C as a function of reducing substrate concentration. ABTS cation radical ($ABTS^{\bullet+}$) formation was followed at 414 nm ($\epsilon_{414\,nm} = 31.1$ mM^{-1} cm^{-1}). The reaction mixture contained 10 nM HRPC, 200 μM H_2O_2, and ABTS at various concentrations in 30 mM sodium phosphate, pH 7.0. Initial steady-state rates were also determined using a chronometric method in which absorbance changes at 414 nm were measured and the initial rates at different ABTS concentrations were calculated from the length of the lag period induced by the presence of ascorbate (see also Results and Discussion).

Steady-State Kinetics of the Reaction of HRPC with o-Diphenols. The chronometric method detailed in the Results and Discussion section was also used to determine the kinetic constants for all of the *o*-diphenols except for epinine, L-isoproterenol, L-dopa, and L-α-methyldopa. Monitoring was at 400 nm (corresponding to the *o*-quinone product) when 4-methylcatechol, 4-*tert*-butylcatechol, *N*-acetyldopamine, DHPPA, DHPAA, pyrogallol, or catechol were assayed and at 475 nm (corresponding to the aminochrome product) when dopamine and L-noradrenaline were assayed. Epinine, L-isoproterenol, L-dopa, and L-α-methyldopa gave *o*-quinones with high cyclization rate constants (*24*−*27*), which prevented significant reduction by ascorbate. Thus, initial steady-state rates were determined following the appearance of the corresponding aminochromes at 490 nm ($\epsilon_{490\,nm} = 2.8 \times 10^3$ M^{-1} cm^{-1}) and at 500 nm ($\epsilon_{500\,nm} = 4.3 \times 10^3$ M^{-1} cm^{-1}) in the case of epinine and L-isoproterenol, respectively, and at 475 nm ($\epsilon_{475\,nm} = 3.6 \times 10^3$ M^{-1} cm^{-1}) in the case of L-dopa or L-α-methyldopa. In all cases, the reaction medium contained 30 mM sodium phosphate, pH 7.0.

Scheme 2

$$\text{HRPC–II} + \text{ABTS} \underset{k'_{-5}}{\overset{k_{+5}}{\rightleftharpoons}} [\text{HRPC–II}\cdot\text{ABTS}] \xrightarrow{k_{+6}} \text{HRPC} + \text{ABTS}^{\bullet+} + \text{H}_2$$

Reaction of Ascorbic Acid with Hydrogen Peroxide. The oxidative degradation of ascorbic acid by H_2O_2 was investigated by observing the decay of ascorbic acid at 290 nm [$\epsilon_{290\ nm} = 2.8 \times 10^3\ M^{-1}\ cm^{-1}$ (*28*)]. Primary plots of v_0 versus [AH_2] at different H_2O_2 concentrations were linear with a slope corresponding to $k_{obs} = k_x[H_2O_2]$. Secondary plots of k_{obs} vs [H_2O_2] gave a straight line, whose slope is the second-order rate constant for the reaction of ascorbate with H_2O_2, k_x.

Kinetic Data Analysis. Pre-steady-state kinetic data were analyzed by fitting the absorbance versus time curves to exponential functions using a least-squares minimization program supplied by Hi Tech Scientific Ltd. The values of the apparent Michaelis constant ($K_m^{app,S}$) and maximum steady-state rate (V_{max}^{app}) for HRPC when ABTS was varied at fixed concentration of H_2O_2 were calculated by triplicate measurements of v_0 at each reducing substrate concentration. The reciprocal of the variances of v_0 were used as weighting factors in the nonlinear regression fitting of v_0 vs [ABTS] data to eq 2. The fitting was carried out by using a Marquardt's algorithm (*29*) implemented in the Sigma Plot 2.01 program for Windows (*30*). Initial estimates of $K_m^{app,S}$ and V_{max}^{app} were obtained from the Hanes−Woolf equation, a linear transformation of the Michaelis equation (*31*). The absolute kinetic constants V_{max} (maximum steady-state rate), $K_m^{H_2O_2}$ (Michaelis constant of HRPC toward hydrogen peroxide), and K_m^S (Michaelis constant of HRPC toward *o*-diphenols) were calculated from primary and secondary plots of $1/v_0$ vs $1/[S]_0$ (eq A8).

NMR Assays. ^{13}C NMR spectra of *o*-diphenols were obtained at pH 7.0 on a Varian Unity spectrophotometer (300 MHz) using ^2H_2O as solvent. Chemical shift values (δ) were measured relative to those for tetramethylsilane ($\delta = 0$). The maximum accepted error for each peak was ±0.03 ppm.

RESULTS AND DISCUSSION

Pre-Steady-State Kinetics of the Reaction of HRPC-II with ABTS. The second-order-rate constants for the reduction of HRPC-II (k_{+5} in Scheme 2) by ABTS has previously been calculated from steady-state kinetic data (*18*). Although the reaction is sufficiently slow for it to be determined by stopped-flow spectrophotometry under pseudo-first-order conditions (>10-fold excess of ABTS), the formation of the intensely colored $ABTS^{\bullet+}$ has previously prevented direct monitoring of HRPC-II reduction in the Soret region. However, we have now been able to monitor this reaction at 423 nm in the presence of a 3-fold molar excess of ascorbate (over ABTS), which rapidly reduces $ABTS^{\bullet+}$ radicals as they are formed (*17*). The absorbance/time curves were biphasic (Figure 1) and could be fitted to a two-exponential function, $A(t) = A_1 \exp(-\lambda_1 t) + A_2 \exp(-\lambda_2 t)$. Under pseudo-first-order conditions with ABTS in large excess over HRPC-II, λ_1 increased linearly with increasing ABTS concentration (0.05−1.0 mM; Figure 1, inset). The second exponential, λ_2, exhibited a hyperbolic dependence on the concentration of ABTS (0.05−1.0 mM; Figure 1, inset). This dependence can be explained if the reaction

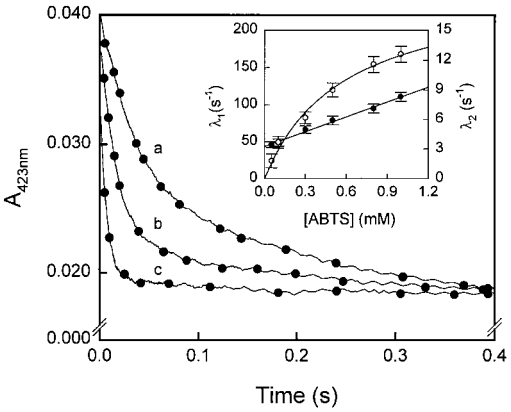

FIGURE 1: Stopped-flow time courses at 423 nm for the reaction of HRPC-II (4.5 μM) with ABTS in 30 mM phosphate buffer, pH 7.0. Curves a−c correspond to 0.1, 0.3, and 0.5 mM ABTS, respectively. In each experiment a 3-fold excess of ascorbic acid over ABTS was used. The filled circles are simulated data points using the rate constant from Table 1 and Scheme 1. Inset: Dependence of apparent first-order rate constants λ_1 (●) and λ_2 (○) for the reaction of HRPC-II with ABTS on [ABTS] at pH 7.0.

between HRPC-II and ABTS occurs by a two-step mechanism where k_{+5} is the second-order rate constant for the binding of ABTS to HRPC-II, k_{-5} is the first-order rate constant for ABTS dissociation from the transient complex, and k_{+6} is the first-order rate constant for electron (and/or coupled proton) transfer step(s) associated with substrate oxidation. Since the plot of λ_2 vs [ABTS] passes through the origin, the second step must be essentially irreversible, as indicated by the omission of k_{-6} from Scheme 2. Initial estimates of the elementary rate constants for the partial reactions of Scheme 2 showed that both steps occur at comparable rates, and so no simplifying assumptions can be made with regard to the rate expressions necessary to obtain the values of the individual rate constants. A mathematical solution was given by Bernasconi (*32*) and the elementary rate constants can be obtained from plots of the sum or the product of the first-order rate constants of the two phases vs [ABTS]. The values of these elementary rate constants are given in Table 1. Simulations of the absorbance versus time curves using these values were made using a computer program written by García-Sevilla et al. (*33*). These are shown overlaid on the stopped-flow data in Figure 1.

Steady-State Kinetics of the Reaction of HRPC with ABTS. Childs and Bardley (*34*) described a complex scheme for ABTS oxidation while Smith et al (*18*) gave a fuller treatment of steady-state data albeit over a limited range of substrate concentrations. These latter authors studied the reaction of both glycosylated and recombinant HRPC with ABTS at pH 5.0, while we have now carried out similar experiments at pH 7.0 (Figure 2) in order to compare pre-steady-state and steady-state results. ABTS is a peroxidase substrate which, when oxidized in the presence of H_2O_2 in a typical peroxidative reaction, generates a metastable radical, $ABTS^{\bullet+}$, with a characteristic absorption spectrum and an absorption maximum at 414 nm. The initial steady-state rate of formation of $ABTS^{\bullet+}$ (v_0) showed a hyperbolic dependence on ABTS concentration (Figure 2A). A conventional ping-pong (ordered two substrates, two products) mechanism assuming dissociation and transformation steps is depicted in Scheme 3 where E, E·H_2O_2, E-I, E-I·S, R, E-II, and E-II·S represent HRPC, the complex HRPC·H_2O_2, HRPC-I, RH_2,

Table 1: Kinetic and Elementary Rate Constants for the Reaction of HRPC and HRPC-II with ABTS at pH 7.0 and 25 °C

method	k_{+5} (M^{-1} s^{-1})	k_{+6} (s^{-1})	k_{cat} (s^{-1})	K_m^S (mM)
		Pre-Steady-State		
stopped flow	$(7.82 \pm 0.61) \times 10^4$	42.1 ± 2.0		0.54 ± 0.08[a]
		Steady-State		
$ABTS^{\bullet+}$ formation	$(7.02 \pm 0.42) \times 10^4$		45.5 ± 2.0	0.64 ± 0.08
chronometric	$(6.70 \pm 0.81) \times 10^4$		45.3 ± 1.8	0.67 ± 0.06

[a] The Michaelis constant of HRPC-II toward ABTS can be calculated according to the expression $K_m = (k_{-5} + k_{+6})/k_{+5}$. Assuming $k_{-5} \ll k_{+6}$, the calculated K_m value is that indicated in this table.

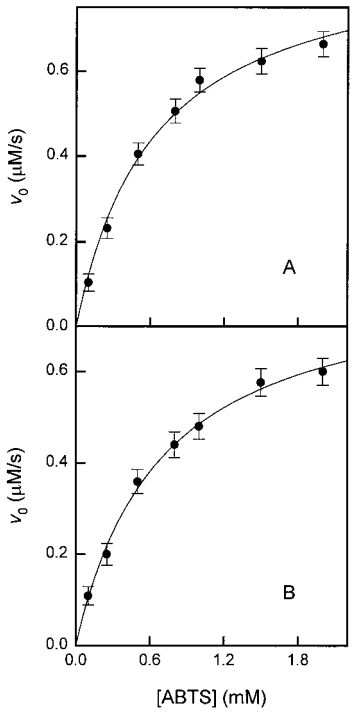

FIGURE 2: Dependence of the steady-state initial rate (v_0) versus [ABTS]. v_0 values were calculated by using the $ABTS^{\bullet+}$ formation (A) or the chronometric method (B). In both cases the reaction mixture contained 2 nM HRPC and 0.2 mM H_2O_2 in 30 mM phosphate buffer (pH 7.0). In panel B, 20 μM ascorbic acid was added to the reaction medium.

Scheme 3

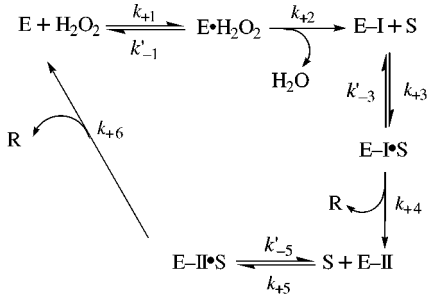

the complex HRPC-I·RH_2, $RH^{\bullet}$, HRPC-II, and the complex HRPC-II·RH_2, respectively. A complete kinetic treatment of Scheme 3 is given in the Appendix. Substitution of eqs A5−A7 into eq A3 (see Appendix) gives the following expression:

$$v_0 = \frac{2k_{cat}[H_2O_2]_0[S]_0[E]_0}{\frac{k_{cat}}{k_{+5}}[H_2O_2]_0 + \frac{k_{cat}}{k_{+1}}[S]_0 + [H_2O_2]_0[S]_0} \quad (1)$$

Note that this equation is obtained from the kinetic analysis of Scheme 3, which includes binding and transformation rate constants for all the enzyme intermediates. Equation 1 can be rearranged to

$$v_0 = \frac{V_{max}^{app}[S]_0}{V_m^{app,S} + [S]_0} \quad (2)$$

where

$$V_{max}^{app} = \frac{2k_{cat}[H_2O_2]_0[E]_0}{(k_{cat}/k_{+1}) + [H_2O_2]_0} \quad (3)$$

$$K_m^{app,S} = \frac{(k_{cat}/k_{+5})[H_2O_2]_0}{(k_{cat}/k_{+1}) + [H_2O_2]_0} \quad (4)$$

The experimental data shown in Figure 2A were fitted to eq 2 by nonlinear regression. The kinetic parameters V_{max}^{app} and $K_m^{app,S}$ were determined, and the values of k_{cat} and k_{+5} were calculated according eqs 3 and 4. The value of k_{+1} (1.7×10^7 M^{-1} s^{-1}) was obtained from stopped-flow measurements as previously described (*13*); the concentration of hydrogen peroxide was 0.2 mM. As can be seen in Table 1, the k_{cat} value is similar to those of k_{+6} obtained from stopped-flow data. These data show that when ABTS is a substrate, the reduction of HRPC-II is rate-limiting (i.e., k_{+2}, $k_{+4} \gg k_{+6}$). In addition, the saturation kinetics observed for ABTS show that reduction of HRPC-II is a two-step process.

Chronometric Method for Determining Peroxidase Steady-State Activity. ABTS is used in peroxidase assays because of its special physicochemical characteristics: high chemical stability, high water solubility, and UV−visible absorption spectrum ($\lambda_{max} = 340$ nm). The reaction product, $ABTS^{\bullet+}$, is a very stable radical, has a high molar extinction coefficient, and is generated directly from its precursor (*34*, *35*). However, kinetic studies with other types of substrate, such as phenolic compounds, are more difficult. This is because many phenolic substrates after oxidation give rise to complex mixtures of polymers with of poorly defined stoichiometry. Therefore, we have developed a chronometric method, which can be used for determining peroxidase activity with a wide class of substrates. We first checked the validity of this method using ABTS as the peroxidase substrate. Ascorbate reduces many radicals and quinones at high rates (5×10^7−2×10^9 M^{-1} s^{-1}) (*36*−*38*). When ascorbate is present in excess, the reaction between ascorbate and the product radical should be the fastest reaction in the system. The reaction between the peroxidase intermediates and substrate should then become rate-limiting. Therefore, the product radical will be reduced back to substrate as

Scheme 4

$$2ABTS^{\bullet+} + 2AH_2 \longrightarrow 2ABTS + 2AH^{\bullet+}$$
$$2AH^{\bullet+} \longrightarrow AH_2 + A$$

rapidly as it is generated by the peroxidase. The stoichiometry of the reaction between ascorbate and ABTS radical is well-known (*39*) (Scheme 4). The overall reaction is $2ABTS^{\bullet+} + AH_2 \rightarrow 2ABTS + A$, where AH_2 is ascorbic acid and A represents dehydroascorbic acid. Therefore, the presence of ascorbate in the peroxidase system gives the following stoichiometry: 1 mol of H_2O_2/2 mol of $ABTS^{\bullet+}$/1 mol of AH_2.

A lag period (τ) is induced in the ABTS assay when AH_2 is present. The value of τ depends on the initial AH_2 concentration. In the absence of AH_2, the measurable concentration of $ABTS^{\bullet+}$ at a given time is

$$[ABTS^{\bullet+}] = v_0 t \quad (5)$$

In the presence of AH_2, the measurable concentration of $ABTS^{\bullet+}$ at a given time is $v_0 t$ minus the amount of $ABTS^{\bullet+}$ reduced by the AH_2 present initially:

$$[ABTS^{\bullet+}] = v_0 t - 2[AH_2] \quad (6)$$

If τ is the time required for the enzyme to produce a concentration of $ABTS^{\bullet+}$ equal to $2[AH_2]$ then

$$v_0 \tau = 2[AH_2] \quad (7)$$

and

$$\tau = 2[AH_2]/v_0 \quad (8)$$

Therefore, τ depends directly on the concentration of ascorbate and on the hydrogen peroxide, ABTS, and HRPC concentrations, as shown by the analytical expression for v_0 (eq A1). Peroxidase activities for ABTS oxidation in the presence of ascorbate can therefore be determined using the following equation:

$$v_0 = 2[AH_2]/\tau \quad (9)$$

However, several factors need to be taken into account if this method is to be used rigorously. First, ascorbic acid may be decomposed by a variety of reactions such as its autoxidation by molecular oxygen. However, under the anaerobic conditions used in the present study, this reaction cannot occur. The most significant degree of ascorbic acid degradation during the assay time will be due to its oxidation by hydrogen peroxide (*40*). This reaction becomes important for long lag periods. The reaction of ascorbic acid with H_2O_2 can be considered as a second-order reaction, whose rate is defined by

$$d[AH_2]/dt = k_x[AH_2][H_2O_2] \quad (10)$$

where k_x is the second-order rate constant for the oxidation of ascorbic acid by H_2O_2, which was calculated to be 1.03 $\pm$ 0.1 M^{-1} s^{-1}. Integrating eq 10 between $t = 0$ ($[AH_2]_0$) and t ($[AH_2]_t$) gives

$$[AH_2]_t = [\boldsymbol{AH}_2]_0 \, e^{-k_x[H_2O_2]t} \quad (11)$$

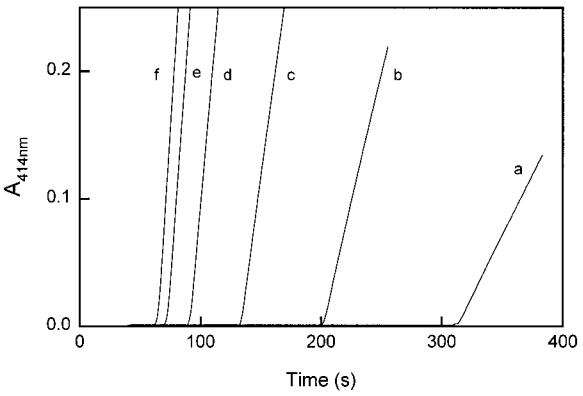

FIGURE 3: Time course of $ABTS^{\bullet+}$ accumulation in the presence of HRPC (2 nM), ascorbic acid (20 μM), H_2O_2 (0.2 mM), and ABTS (curves a−f correspond to 0.1, 0.25, 0.5, 1.0, 1.5, and 2.0 mM) in phosphate buffer (pH 7.0).

For short times $e^{-k_x[H_2O_2]t} \approx 1 - k_x[H_2O_2]\tau$ and by substituting into eq 9:

$$v_0 = \frac{2[AH_2](1 - k_x[H_2O_2]\tau)}{\tau} \quad (12)$$

Equation 12 can be used for the accurate determination of v_0 at different concentrations of reducing substrates. The reaction between ascorbate and HRPC-II ($k = 10^3$ M^{-1} s^{-1}) can be minimized by using a low concentration of ascorbate (typically less than a 10% of the initial concentration of hydrogen peroxide). This also ensures a low consumption of H_2O_2, which is a necessary condition for steady-state determinations. Figure 3 shows the time courses of $ABTS^{\bullet+}$ formation at different concentrations of ABTS using this chronometric method. The dependence of v_0 on ABTS concentration is shown in Figure 2B. The direct monitoring of $ABTS^{\bullet+}$ formation and the chronometric method gave very similar values for the kinetic and elementary rate constants shown in Table 1.

Steady-State Kinetics of the Reaction of HRPC with o-Diphenols. HRPC catalyzes the oxidation of various aromatic secondary metabolites, hydroquinones, and catechols by H_2O_2 to the corresponding quinones by a well-characterized, peroxidative, one-electron transfer mechanism. The peroxidative oxidation of *o*-diphenols (*o*-D) by HRPC has been studied by ESR spin stabilization (*41*, *42*). This involves *o*-semiquinone (*o*-SQ) as the primary one-electron oxidation product. *o*-SQ then undergoes either a disproportion reaction with another *o*-SQ molecule or a nonenzymatic aerobic oxidation (*43*, *44*). Both processes produce the corresponding *o*-quinone (*o*-Q). The latter possibility was avoided in our experiments by the use of anaerobic conditions. In the case of catecholamines, deprotonation of the amine side chain causes the *o*-Q to undergo a 1,4 intramolecular cyclation to form leucoadrenochrome, which may be rapidly oxidized to adrenochrome (*45*). Another problem with steady-state kinetic determinations of this type of substrate is the redox reaction of *o*-Q with *o*-D, which becomes important when the concentration of reducing substrate has to be increased to reach saturation kinetics. Reactions of this type have produced kinetic artifacts such as the apparent inhibition of tyrosinase by an excess reducing substrate (*46*).

In our peroxidase system, ascorbic acid can react either with *o*-SQ or *o*-Q according to the chain reactions in Schemes

Scheme 5

$$2o\text{–}SQ + 2AH_2 \longrightarrow 2o\text{–}D + 2AH^{\bullet+}$$
$$2AH^{\bullet+} \longrightarrow AH_2 + A$$

Scheme 6

$$2o\text{–}SQ \longrightarrow o\text{–}Q + o\text{–}D$$
$$o\text{–}Q + AH_2 \longrightarrow o\text{–}D + A$$

5 or 6. Thus, when ascorbic acid is present, the same stoichiometry, 1 mol of H_2O_2/2 mol of *o*-SQ/1 mol of AH_2, is expected in both cases (Schemes 5 and 6). Therefore, eq 12 can be used for initial steady-state rate determinations. Although phenoxyl radicals are known to react rapidly with ascorbate, the reaction between *o*-SQ and ascorbate was reported to be slow (*36*). This together with the fact that catecholamines with a fast cyclization rate constant, such as epinine, L-isoproterenol, L-dopa, and L-α-methyldopa, are not reduced by ascorbate suggest that ascorbic acid reduces at the level of *o*-Q (Scheme 6).

Using the chronometric method described above, we have studied the effect of the concentration of several *o*-diphenols on v_0. Hyperbolic dependencies (Figure 4) were observed for all the substrates assayed, except for L-dopa and L-α-methyldopa. Since saturation kinetics were not observed for these two latter substrates, we concluded that K_m^S values could not be measured, and only the calculation of k_{+5} was possible (Table 3). For all the other substrates, we obtained a linear dependence of experimental $1/v_0$ values versus $1/[S]_0$ at different concentrations of hydrogen peroxide (data not shown). The straight lines obtained were essentially parallel since, according to eq A8, the slopes are independent of $[S]_0$. Secondary plots of the *y*-axis ordinate obtained from primary plots versus $1/[H_2O_2]_0$ gave straight lines according eq A9. The kinetic constants calculated using this analysis for all the *o*-diphenols used are given in Table 2. For some of the substrates, the ordinate intercepts obtained from the primary plots were independent of hydrogen peroxide concentration, and so their $K_m^{H_2O_2}$ values could not be determined. These data show that the value of $K_m^{H_2O_2}$ depends on the nature of the reducing substrate. This dependence could have been predicted from eq A7 since $K_m^{H_2O_2}$ is directly related to k_{cat}, which includes the first-order rate constant for the electron transfer of the substrate to HRPC-II (k_{+6}). This relationship is observed in Figure 5, where k_{+1} can be calculated from the inverse of the slope according to eq A7. The calculated value ($k_{+1} = 1.69 \times 10^7$ M^{-1} s^{-1}) agrees with the value previously measured by stopped-flow spectrophotometry [1.7×10^7 M^{-1} s^{-1} (*13*)]. The kinetic parameters V_{max}, K_m^S, and $K_m^{H_2O_2}$ for the HRPC-catalyzed oxidation of several *o*-diphenol substrates are given in Table 2. This table also includes the values of k_{cat} calculated according eq A5. Unexpectedly, 4-methylcatechol, TBC, pyrogallol, and catechol showed, within experimental error, the same k_{cat} value of ca. 2.17×10^3 s^{-1}.

Factors Controlling the Binding of Reducing Substrates to HRPC. In general, the rates of reaction of each of the peroxidase intermediates with a given substrate are so fast that stopped-flow or similar methods are required to measure the rate constant for each individual step of the catalytic cycle. Often saturation kinetics are not observed using stopped-flow methods because the substrate concentrations necessary to maintain the rate within the stopped-flow range ($k_{obs} < 1000$ s^{-1}) are too low. Since the reaction of HRPC-II with a reducing substrate occurs by the two-step mechanism described in Scheme 2, the observed rate constant has the following expression: $k_{obs} = k_{+6}[S]/K_m^S + [S]$ where $K_m^S = k_{+6}/k_{+5}$ assuming $k_{+6} \gg k_{-5}$. Therefore, in conventional stopped-flow experiments with $[S] \ll K_m^S$, the rate-limiting step is the second-order rate constant for the binding of the reducing substrate to HRPC-II, k_{+5} (k_c in Scheme 1). Comparison of this second-order rate constants for the binding of ABTS to HRPC-I and HRPC-II gives information on the nature of the interaction between substrate and both enzyme intermediates. Thus, ABTS binds to HRPC-I with a second-order rate constant ca. 2×10^6 M^{-1} s^{-1} (*17*), 30 times faster than to HRPC-II (Table 1). The origin of this significant difference in rate is intriguing considering the previously assumed structural similarities between HRPC-I and HRPC-II.

Table 3 shows a range of 3 orders of magnitude for the second-order rate constant (k_{+5}) for the oxidation of *o*-diphenols used in this study (values calculated according to eq A6). The value of k_{+5} is higher for hydrophobic substrates than for those with a charged side chain. These data are therefore best explained in terms of polar effects and to a lesser extent steric hindrance, as has been previously proposed for *o*-substituted phenols (*47*). Since 4-*tert*-butylcatechol, 4-methylcatechol, and catechol have k_{+5} values within a factor of 2 of each other, the binding site on HRPC must be able to accommodate bulky, hydrophobic side chains at the 4 position on the substrate. However, the most polar and bulky *o*-diphenols in this study, L-dopa and L-α-methyldopa, are the poorest substrates of HRPC both in terms of rates of binding and oxidation.

N-Acetyldopamine, despite its relatively bulky side chain, has a k_{+5} value similar to that of 4-methylcatechol (Table 3). Its side chain resembles that of BHA in terms of the NH−CO group. BHA reacts with HRPC-II with a second-order rate constant of 7.8×10^5 M^{-1} s^{-1} (*48*), similar to that found for *N*-acetyldopamine (1.29×10^6 M^{-1} s^{-1}). Recently, the crystal structure of the HRPC−BHA complex was determined at 2.0 Å resolution (*49*). The aromatic ring of BHA is surrounded by a hydrophobic pocket, which is formed by His42, Phe68, Gly69, Ala140, Phe141, and Phe179 and heme C18, C-18-methyl, and C-20. The closest aromatic residue to the BHA is Phe179. In the ferric enzyme, the hydrophilic side chain of BHA makes hydrogen bonds with the two distal residues involved in catalysis His42 (BHA O6−His42$N_{\epsilon 2}$ distance 2.8 Å) and Arg38 (BHA O5−Arg38$N_{\eta 2}$ distance 2.9 Å). Additional hydrogen bonds are formed between a backbone oxygen (BHA N33−Pro139O distance 2.7 Å), and with two solvent molecules above the heme iron (BHA O5-water distance 2.6 Å and BHA O6-water distance 3.1 Å). Similar interactions between HRPC-II and the side chain of *N*-acetyldopamine could explain the high k_{+5} value of this substrate. This hydrogen bonding potential with the active site residues of the distal heme pocket suggests that *N*-acetyldopamine is, like BHA, an atypical reducing substrate of HRPC (*49*). Clearly the kinetics of substrate binding, orientation of the substrate at the active site, and closeness of approach to the heme edge (a key determinant of electron-transfer rate) will depend on the nature (polar or hydropho-

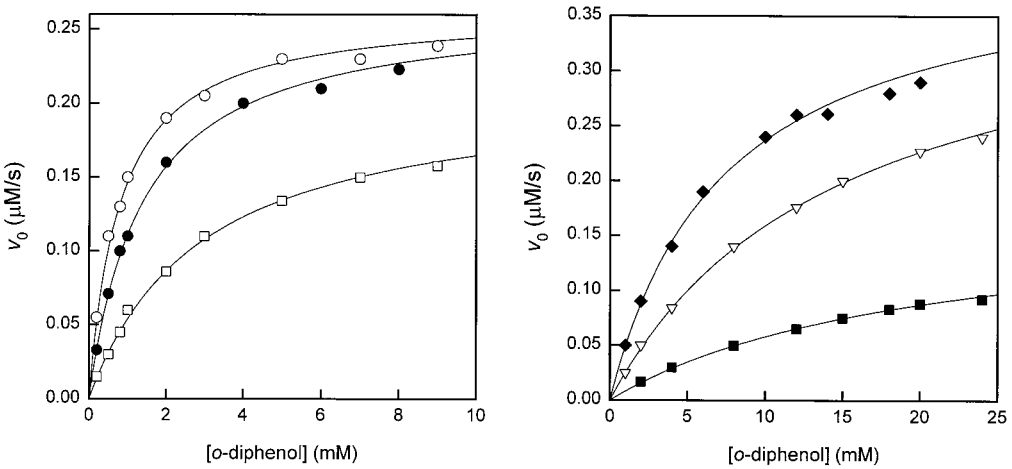

FIGURE 4: Hyperbolic dependence of v_0 vs [*o*-diphenol]. v_0 values were obtained by the chronometric method using 20 μM ascorbic acid and 0.2 mM H_2O_2 in 30 mM phosphate buffer (pH 7.0). (A) Plot for (●) catechol, (○) 4-methylcatechol, and (□) DHPPA assayed with 1 nM HRPC. (B) Plot for (◆) DHPAA, (▽) dopamine, and (■) L-noradrenaline assayed with 0.5 nM HRPC.

Table 2: Steady-State Kinetic Constants for the Reaction of HRPC with *o*-Diphenols[a]

o-diphenol	V_{max} (μM/s)	k_{cat} (s^{-1})	K_m^S (mM)	$K_m^{H_2O_2}$ (μM)
4-methylcatechol	4.31 ± 0.20	2155 ± 105	1.3 ± 0.1	128 ± 8
catechol	4.40 ± 0.30	2200 ± 150	2.3 ± 0.1	129 ± 8
TBC	4.29 ± 0.20	2146 ± 100	2.6 ± 0.2	125 ± 7
pyrogallol	4.36 ± 0.4	2180 ± 130	4.9 ± 0.5	127 ± 10
N-acetyldopamine	3.60 ± 0.15	1800 ± 75	1.4 ± 0.1	112 ± 6
DHPPA	3.12 ± 0.12	1558 ± 120	4.3 ± 0.3	97.4 ± 5
DHPAA	0.94 ± 0.10	469 ± 49	8.4 ± 0.6	34.4 ± 5
epinine	0.90 ± 0.10	451 ± 51	20.6 ± 1.0	25.9 ± 4
dopamine	0.89 ± 0.08	447 ± 42	16.8 ± 1.3	27.3 ± 4
L-isoproterenol	0.37 ± 0.03	186 ± 16	21.5 ± 1.2	
L-noradrenaline	0.34 ± 0.04	172 ± 22	8.1 ± 0.7	

[a] Conditions were 30 mM phosphate buffer, pH 7.0, and 1 nM HRPC. Results are means ± SD for three separate experiments.

Table 3: Steady-State Kinetic Constants for the Reaction of HRPC with *o*-Diphenols[a]

o-diphenol	k_{+5} ($M^{-1}s^{-1}$)	k_{+6} (s^{-1})	δ_3 (ppm)	δ_4 (ppm)
4-methylcatechol	$(1.66 \pm 0.20) \times 10^6$	$> 2.0 \times 10^4$	146.43	144.06
catechol	$(9.56 \pm 1.06) \times 10^5$	$> 2.0 \times 10^4$	146.59	146.59
TBC	$(8.25 \pm 1.02) \times 10^5$	$> 2.0 \times 10^4$	146.24	144.07
pyrogallol	$(4.48 \pm 0.51) \times 10^5$	$> 2.0 \times 10^4$	146.7	138.00
N-acetyldopamine	$(1.29 \pm 0.15) \times 10^6$	1.06×10^4	146.44	144.82
DHPPA	$(3.62 \pm 0.53) \times 10^5$	5.52×10^3	146.58	144.85
DHPAA	$(5.58 \pm 0.98) \times 10^4$	5.98×10^2	146.59	145.51
Epinine	$(2.19 \pm 0.35) \times 10^4$	5.69×10^2	146.81	145.66
dopamine	$(2.66 \pm 0.45) \times 10^4$	5.63×10^2	146.86	145.66
L-isoproterenol	$(8.65 \pm 1.22) \times 10^3$	2.04×10^2	146.88	146.83
L-noradrenaline	$(2.12 \pm 0.45) \times 10^4$	1.87×10^2	146.88	146.88
L-dopa	$(1.12 \pm 0.20) \times 10^3$		146.83	145.98
L-α-methyldopa	$(9.30 \pm 0.31) \times 10^2$		146.67	146.13

[a] Conditions were 30 mM phosphate buffer, pH 7.0, and 1 nM HRPC. Results are means ± SD for three separate experiments.

bic) and size of the side chain. The ability to form hydrogen bonding interactions, as demonstrated for BHA by X-ray crystallography, may also be important. The peripheral hydrophobic patch in HRPC should favor the access of hydrophobic *o*-diphenols to the binding site. Thus 4-methylcatechol, catechol, and TBC are more likely to bind with their hydrophobic side chains orientated toward the hydrophobic pocket formed by Phe179, Phe68, Pro141, Ala140, and Gly69 and heme C18, C-18-methyl, and C-20 (*49*, *50*).

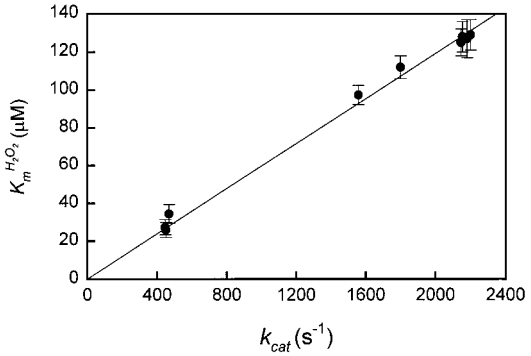

FIGURE 5: Dependence of $K_m^{H_2O_2}$ vs k_{cat} values for different *o*-diphenolic substrates. Data are presented in Table 2.

However, *o*-diphenols with a polar side chain may bind in a different orientation that maximizes hydrogen bond formation. This is likely to be a major factor in controlling electron-transfer rates from the bound substrate to the ferryl heme in compound II (k_{+6}).

Assignment of the First-Order Rate-Limiting Constant (k_{+6}) for the Reaction of HRPC with o-Diphenol Substrates. Electron donation to the electron-deficient porhpyrin π-cation radical of HRPC-I is accompanied by addition of a single proton to the protein (*6*). For HRPC-II, the electron is transferred to the ferryl group at the center of the porphyrin in a reaction coupled to two proton transfers to the ferryl oxygen atom to give water as a leaving group. Recent data (*51*, *52*) have indicated that the proton transfer does not occur in the rate-limiting step, but rather that the reaction is kinetically controlled by electron transfer. The data presented in Table 2 are not consistent with k_{cat} being the rate of product dissociation because, if this were so, k_{cat} would be expected to be faster for hydrophilic than for hydrophobic substrates. Therefore, we suggested that this first order-rate constant corresponds to electron transfer from the substrate to either the protein or, more likely, directly to the heme (*53*). Since there is a correlation between NMR ^{13}C chemical shift values (δ) and electronic density at the carbon atom (*54*, *55*), it is not surprising that a linear correlation between δ values and σ has also been reported (*56*). We therefore determined the δ_3 and δ_4 values for the *o*-diphenols used in the present study in order to correlate these with oxidation rates. The δ_3 and δ_4 values for all the *o*-diphenols were very low (Table 3).

The oxygen atoms of the hydroxyl groups at C-3 and C-4 in these *o*-diphenols must have relatively high electron density. Since the electron density at C-4 is higher than that at C-3 ($\delta_3 > \delta_4$), the electron transfer in HRPC-II is presumably from the oxygen atom at the para position to the ferryl group. The k_{cat} values for the diphenol substrates, except for catechol, correlate reasonably well with their δ_4 values (Tables 2 and 3). Interestingly, catechol has essentially the same k_{cat} value as pyrogallol, 4-*tert*-butylcatechol, and 4-methylcatechol (Table 2). This may be because the expression for k_{cat} [$k_{cat} = k_{+2}k_{+6}/(k_{+2} + k_{+6})$] is a function of two first-order rate constants, the heterolytic cleavage of the O−O bond of hydrogen peroxide (k_{+2}), and the electron transfer from the reducing substrate to compound II (k_{+6}). Thus, if $k_{+2} \ll k_{+6}$, the expression for the catalytic constant is simplified to $k_{cat} = k_{+2}$, and so the k_{cat} would essentially be independent of the nature of the reducing substrate. This effect has been reported for the oxidation of substrates by the His42Leu HRPC variant (*14*). His42 is thought to act as an acid−base catalyst during the heterolytic cleavage of hydrogen peroxide by HRPC. Therefore, replacing it by leucine makes k_{+2} rate-limiting in the oxidation of reducing substrates. The value of $k_{+2} = 2170\ s^{-1}$ (average of k_{cat} for the first four entries in Table 3) is not very different from those that can be indirectly calculated from the data of Baek and Van Wart (*11*). These authors studied the reaction of HRPC with hydrogen peroxide by stopped-flow cryoenzymology. They proposed a value of $K_m^{H_2O_2} = 46\ \mu M$ when extrapolated to 25 °C. In the absence of reducing substrate, $K_m^{H_2O_2} = (k_{-1} + k_{+2})/k_{+1}$. Therefore, assuming that $k_{-1} \ll k_{+2}$ and $k_{+1} = 1.7 \times 10^7\ M^{-1}\ s^{-1}$, a value of 780 s^{-1} can be calculated for k_{+2}. It is quite reasonable that $k_{+6} > k_{+2}$ for good peroxidase substrates with electron transfer occurring faster than the heterolytic cleavage of bound peroxide. Thus, the values of k_{+6} for 4-methylcatechol, TBC, pyrogallol, and catechol must be at least an order of magnitude higher than k_{+2} for it to be make a negligible contribution in the expression for k_{cat}. However, assuming the value of k_{+2} previously calculated (2170 s^{-1}), the value of k_{+6} for the other *o*-diphenols can be obtained (Table 3). These values show an excellent correlation with δ_4 values. The high value of k_{+6} predicted for pyrogallol can be explained by its low δ_4 value. The high value obtained for catechol, which has a very high δ_4 value, can be explained if it binds optimally to the active site of HRPC-II. Thus, the distances for electron transfer could be optimal in the case of substrates with a hydrophobic side chain. The differential behavior of phenol and aniline derivatives during oxidation by HRPC has also been explained in terms of the different distances and orientations of these substrates with respect to the ferryl group of HRPC-II (*57*).

In conclusion, the reaction of HRPC-II with *o*-diphenols has been shown to occur by a two-step mechanism in which the first step corresponds to the formation of an enzyme−substrate complex, and the second step corresponds to the electron transfer from the substrate to the iron atom. The size and hydrophobicity of these substrates control their access to the hydrophobic binding site of HRPC. Electron density in the hydroxyl group of C-4 and its distance to the ferryl oxygen atom are key determinants of the rate of electron transfer.

APPENDIX

The conventional ping-pong mechanism (ordered two substrates, two products), assuming dissociation and transformation steps, is depicted in Scheme 3. To analyze the kinetic data corresponding to initial rate of radical production, v_0, the following equation was derived:

$$v_0 = \frac{\alpha_1[H_2O_2]_0[S]_0[E]_0}{\beta_1[H_2O_2]_0 + \beta_2[S]_0 + \beta_3[H_2O_2]_0[S]_0} \quad \text{(A1)}$$

where the coefficients α_1 and $\beta_1-\beta_3$ are as follows:

$$\alpha_1 = 2k_{+1}k_{+2}k_{+3}k_{+4}k_{+5}k_{+6}$$

$$\beta_1 = k_{+1}k_{+2}k_{+5}k_{+6}(k_{-3} + k_{+4}) + k_{+1}k_{+2}k_{+3}k_{+4}(k_{-5} + k_{+6})$$

$$\beta_2 = k_{+3}k_{+4}k_{+5}k_{+6}(k_{-1} + k_{+2})$$

$$\beta_3 = k_{+1}k_{+3}k_{+4}k_{+5}k_{+6} + k_{+1}k_{+2}k_{+3}k_{+5}k_{+6} + k_{+1}k_{+2}k_{+3}k_{+4}k_{+5} \quad \text{(A2)}$$

In deriving the steady-state rate of radical product formation, it has been assumed that the free enzyme is limiting, i.e., that the initial concentration of hydrogen peroxide and S (reducing substrate), $[H_2O_2]_0$ and $[S]_0$, are much higher than that of the free enzyme (HRPC), $[E]_0$, and that the reaction time is such that it the concentrations of the substrates remain essentially constant.

Equation 1 can be rewritten as

$$v_0 = \frac{V_{max}[H_2O_2]_0[S]_0}{K_m^S[H_2O_2]_0 + K_m^{H_2O_2}[S]_0 + [H_2O_2]_0[S]_0} \quad \text{(A3)}$$

If in the mechanism shown in Scheme 2 we assume the following relationships (*6*, *18*, *58*):

$$k_{+2} \gg k_{-1}$$

$$k_{+4} \gg k_{-3}$$

$$k_{+6} \gg k_{-5}$$

$$k_{+3} \gg k_{+5}$$

$$k_{+4} \gg k_{+2}, k_{+6} \quad \text{(A4)}$$

the analytical expression for V_{max} (maximum steady-state rate), K_m^S (Michaelis constant of HRPC toward *o*-diphenol), and $K_m^{H_2O_2}$ (Michaelis constant of HRPC toward hydrogen peroxide) are given after rearrangement by

$$V_{max} = \alpha_1[E]_0/\beta_3 = 2k_{+2}k_{+6}[E]_0/(k_{+2} + k_{+6}) = 2k_{cat}[E]_0 \quad \text{(A5)}$$

$$K_m^S = \beta_1/\beta_3 = k_{+2}k_{+6}/[k_{+5}(k_{+2} + k_{+6})] = k_{cat}/k_{+5} \quad \text{(A6)}$$

$$K_m^{H_2O_2} = \beta_2/\beta_3 = k_{+2}k_{+6}/[k_{+1}(k_{+2} + k_{+6})] = k_{cat}/k_{+1} \quad \text{(A7)}$$

The reciprocal plot of $1/v_0$ vs $1/[S]_0$ has the following expression:

$$\frac{1}{v_0} = \frac{K_m^S}{V_{max}} \frac{1}{[S]_0} + \frac{K_m^{H_2O_2}}{V_{max}} \frac{1}{[H_2O_2]_0} + \frac{1}{V_{max}} \qquad \text{(A8)}$$

where the *y*-axis intercept of the primary plots vs $1/[H_2O_2]_0$ has the following expression:

$$y\text{-axis} = \frac{K_m^{H_2O_2}}{V_{max}} \frac{1}{[H_2O_2]_0} + \frac{1}{V_{max}} \qquad \text{(A9)}$$

From primary and secondary plots of $1/v_0$ vs $1/[S]_0$ and the *y*-axis intercept of the primary plots vs $1/[H_2O_2]_0$, the kinetic constants for the reaction of HRPC with reducing substrates can be calculated.

REFERENCES

1. Dunford H. B. (1999) in *Heme Peroxidases*, pp 92−97, Wiley-VCH, New York.
2. Klibanov, A. M., Tu, T., and Scott, K. P. (1983) *Science 221*, 259−261.
3. Wada, S., Ichikawa, H., and Tatsumi, K. (1995) *Biotechnol. Bioeng. 45*, 304−309.
4. Buchanan, I. D., and Nicell, J. A. (1997) *Biotechnol. Bioeng. 54*, 251−261.
5. Tatsumi, K., Wada, S., and Ichikawa, H. (1996) *Biotechnol. Bioeng. 51*, 126−130.
6. Dunford, H. B. (1991) in *Peroxidases in Chemistry and Biology* (Everse, J., Everse, K. E., and Grisham, M. B., Eds.) Vol. 2, pp 1−24, CRC Press, Boca Raton, FL.
7. Dunford, H. B., and Stillman, J. S. (1976) *Coord. Chem. 19*, 187−251.
8. Chance, B. (1943) *J. Biol. Chem. 151*, 553−567.
9. Brill, A. S. (1966) *Compr. Biochem. 14*, 447−477.
10. Wang, W., Noël, S., Desmadril, M., Gueguen, J., and Michon, T. (1999) *Biochem. J. 340*, 329−336.
11. Baek, H. K., and Van Wart, H. E. (1989) *Biochemistry 28*, 5714−5719.
12. Baek, H. K., and Van Wart, H. E. (1992) *J. Am. Chem. Soc 114*, 718−725.
13. Rodriguez-Lopez, J. N., Smith, A. T., and Thorneley, R. N. F. (1996) *J. Biol. Chem. 271*, 4023−4030.
14. Rodriguez-Lopez, J. N., Smith, A. T., and Thorneley, R. N. F. (1996) *J. Biol. Inorg. Chem. 1*, 136−142.
15. Newmyer, S. L., and Ortiz de Montellano, P. R. (1995) *J. Biol. Chem. 270*, 19430−19438.
16. Howes, B. D., Rodriguez-Lopez, J. N., Smith, A. T., and Smulevich, G. (1997) *Biochemistry 36*, 1532−1543.
17. Goodwin, D. C., Yamazaki, I., Aust, S. D., and Grover, T. A. (1995) *Anal. Biochem. 231*, 333−338.
18. Smith, A. T., Sanders, S. A., Thorneley, R. N. F., Burke, J. F., and Bray, R. R. C. (1992) *Eur. J. Biochem. 207*, 507−519.
19. Critchlow, J. E., and Dunford, H. B. (1972) *J. Biol. Chem. 247*, 3703−3713.
20. Schonbaum, G. R., and Lo, S. (1972) *J. Biol. Chem. 247*, 3353−3360.
21. Cotton, M. L., and Dunford, H. B. (1973) *Can. J. Chem. 51*, 582−587.
22. Ros, J. R., Rodriguez-Lopez, J. N., and García-Cánovas, F. (1993) *Biochem. J. 295*, 309−312.
23. Patel, P. K., Mondal, M. S., Modi, S., and Behere, D. V. (1997) *Biochim. Biophys. Acta 1339*, 79−87.
24. Jimenez, M., Garcia-Carmona, F., Garcia-Canovas, F., Iborra, J. L., and Lozano, J. A. (1985) *Int. J. Biochem. 17*, 885−890.
25. Jimenez, M., Garcia-Canovas, F., Garcia-Carmona, F., Iborra, J. L., and Lozano, J. A. (1985) *Biochem. Int. 11*, 51−59.
26. Jimenez, M., Garcia-Canovas, F., Garcia-Carmona, F., Tudela, J., and Iborra, J. L. (1986) *Int. J. Biochem. 18*, 39−47.
27. Garcia-Carmona, F., Garcia-Canovas, F., Iborra, J. L., and Lozano, J. A. (1982) *Biochim. Biophys. Acta 717*, 124−131.
28. Chen, G. X., and Asada, K. (1989) *Plant Cell Biol. 30*, 987−998.
29. Marquardt, D. W. (1963) *J. Soc. Ind. Appl. Math. 11*, 431−441.
30. Jandel Scientific. (1994) *Sigma Plot 2.01 for Windows*, Jandel Scientific, Corte Madera.
31. Wilkinson, G. N. (1961) *Biochem. J. 80*, 324−332.
32. Bernasconi, C. F. (1976) *Relaxation Kinetics*, Academic Press, New York.
33. Garcia, R., and Varon, R. (2000) *BioSystems 54*, 151−164.
34. Childs, R. E., and Bardsley, W. G. (1975) *Biochem. J. 145*, 93−103.
35. Arnao, M. B., Acosta, M., del Rio, J. A., Varón, R., and Garcia-Canovas, F. (1990) *Biochim. Biophys. Acta 1041*, 43−57.
36. Schuler, R. H. (1977) *Radiat. Res. 69*, 417−433.
37. Pelizzetti, E., Meisel, D., Mulac, W. A., and Neta, P. (1979) *J. Am. Chem. Soc. 101*, 6954−6959.
38. Bahnemann, D., Asmus, K. D., and Willson, R. L. (1983) *J. Chem. Soc, Perkin Trans. 2*, 1669−1673.
39. Arnao, M. B., Cano, A., Hernandez-Ruiz, J., Garcia-Canovas, F., and Acosta, M. (1996) *Anal. Biochem. 236*, 255−261.
40. Deutsch, J. C. (1998) *Anal. Biochem. 255*, 1−7.
41. Kalyanaraman, B., and Sealy, R. C. (1982) *Biochem. Biophys. Res. Commun. 106*, 1119−1125.
42. Kalyanaraman, B., Felix, C. C., and Sealy, R. C. (1984) *J. Biol. Chem. 259*, 354−358.
43. Sawada, Y., Iyanogi, T., and Yamazaki, I. (1975) *Biochemistry 14*, 3761−3764.
44. Adak, S., Bandyopadhyay, U., Bandyopadhyay, D., and Banerjee, R. K. (1998) *Biochemistry 37*, 16922−16933.
45. Garcia-Canovas, F., Garcia-Carmona, F., Vera, J., Iborra, J. L., and Lozano, J. A. (1982) *J. Biol. Chem. 257*, 8738−8744.
46. Zawistowski, J., Biliaderis, C. G., and Michael Eskin, N. A. (1991) in *Oxidative Enzymes in Foods* (Robinson, D. S., and Eskin, N. A. M., Eds.) pp 217−273, Elsevier Science, London.
47. Dunford, H. B., and Adeniran, A. J. (1986) *Arch. Biochem. Biophys. 251*, 536−542.
48. Aviran, I. (1981) *Arch. Biochem. Biophys. 212*, 483−490.
49. Henriksen, A., Schuller, D. J., Meno, K., Welinder, K. G., Smith, A. T., and Gajhede, M. (1998) *Biochemistry 37*, 8054−8060.
50. Gajhede, M., Schuller, D. J., Henriksen, A., Smith, A. T., and Smith, A. T. (1997) *Nat. Struct. Biol. 4*, 1032−1038.
51. Candeias, L. P., Folkes, L. K., and Wardman, P. (1997) *Biochemistry 36*, 7081−7085.
52. Folkes, L. K., and Candeias, L. P. (1998) *FEBS Lett. 412*, 305−308.
53. Garcia-Moreno, M., Moreno-Conesa, M., Rodriguez-Lopez, J. N., Garcia-Canovas, F. and Varón, R. (1999) *Biol. Chem. 380*, 689−694.
54. Günther, H. (1980) Nuclear magnetic resonance of fluorine-19 and carbon-13. In *NMR Spectroscopy*, pp 364−374. John Wiley and Sons, New York.
55. Farnun, D. G. (1975) Charge density-NMR chemical shift correlations in organic ions. In *Advances in Physical Organic Chemistry* (Gold, V., and Bethell, D., Eds.) Vol. 11, pp 123−173, Academic Press, New York.
56. Shogo, T., Shogo, S., Tomihiro, N., and Fukiko, Y. (1993) *Bull. Chem. Soc. Jpn. 66*, 299−304.
57. Van Haandel, M. J. H., Claassens, M. M. J., Van der Hout, N., Boersma, M. G., Vervoort, J., and Rietjens, I. M. C. M. (1999) *Biochim. Biophys. Acta 1435*, 22−29.
58. Job, D., and Dunford, H. B. (1976) *Eur. J. Biochem. 66*, 607−614.

BI001150P